Diffusion in Laminar Rayleigh-Bénard Convection: Boundary Layers Versus Boundary Tubes

A. M. Dykhne* M. B. Isichenko† and W. Horton
Institute for Fusion Studies
The University of Texas at Austin
Austin, Texas 78712

Abstract

We present new results on the advection-diffusion of a passive tracer in a periodic system of hexagonal Rayleigh-Bénard convection cells at high Péclet number $P = Lv/D_0 \gg 1$, where L is the characteristic length scale of the flow, v the velocity amplitude, and D_0 the molecular diffusivity. We show that the transport properties of this three-dimensional laminar flow are drastically different from those of the well-studied two-dimensional convection rolls. The 3D topology of the streamlines in the hexagonal convection leads to to the formation of boundary tubes near the axes and the edges of the hexagons, in addition to the standard boundary layers found near the faces and the bases. While in the convection rolls and many other flows the boundary-layer-controlled effective diffusivity is enhanced against the molecular diffusivity by a factor involving a positive power of the Péclet number P, we provide a scaling argument that the transport enhancement due to the hexagonal cells is controlled by the boundary tubes and scales only logarithmically with P. This conclusion is confirmed by

*Permanent address: Troitsk Innovation and Thermonuclear Research Institute, 142092 Troitsk, Moscow Region, Russia
†Also at Russian Research Center *Kurchatov Institute*, 123182 Moscow, Russia

a test-particle computation. On the other hand, we find that the subdiffusive regimes of transport in hexagons are similar to those found in other flows with constrained streamlines. The described effects can be used for the experimental investigation of structures in thermal convection.

1 Introduction

Since the early work of Taylor [1] and Richardson [2] it has been realized that convection processes play an important role in transport of various physical agents such as temperature, humidity, salinity, and the like. The advection-diffusion transport is often reducible to a renormalized, or effective diffusion, which has been a subject of considerable interest in fluids [3, 4, 5, 6, 7, 8], plasmas [9, 10], astrophysics [11, 12], and semiconductors [13, 14]. In the case of a steady convection velocity field the advection-diffusion transport is characterized by a single nondimensional parameter — the Péclet number

$$P = \frac{\sqrt{\langle \boldsymbol{\psi}^2(\mathbf{x}) \rangle}}{D_0} , \tag{1}$$

where $\boldsymbol{\psi}$ is the vector potential of the incompressible velocity field $\mathbf{v}(\mathbf{x}) = \boldsymbol{\nabla} \times \boldsymbol{\psi}(\mathbf{x})$ and D_0 the molecular diffusion coefficient. If the vector potential $\boldsymbol{\psi}$ is bounded and therefore the Péclet number (1) is finite, the underlying transport equation,

$$\frac{\partial n}{\partial t} + \boldsymbol{\nabla} \cdot [n\mathbf{v}(\mathbf{x})] = D_0 \boldsymbol{\nabla}^2 n , \tag{2}$$

is reducible [15, 16] to the form of effective difusion,

$$\frac{\partial \langle n \rangle}{\partial t} = \frac{\partial}{\partial x_i} D^*_{ij} \frac{\partial \langle n \rangle}{\partial x_j} , \tag{3}$$

where the effective diffusivity $D^*(\mathbf{l}) = D^*_{ij} l_i l_j / |\mathbf{l}^2|$ in the given direction of $\mathbf{l}$ scales as

$$D^* = D_0 f(P) . \tag{4}$$

The molecular diffusivity D_0 is usually very small, so one is interested in the limit of a large Péclet number. As the effective diffusivity is always greater than D_0 [3], the asymptotics of D^*/D_0 is typically a positive power of P,

$$f(P) = \text{const } P^\alpha , \quad P \gg 1 , \tag{5}$$

where the exponent α depends on the topology of the flow. In general, $0 \leq \alpha \leq 2$ [16]. The familiar examples include $\alpha = 2$ for a shear flow with extended streamlines [4], $\alpha = 1/2$ for convection rolls with the free-slip boundary condition [11], $\alpha = 1/3$ for no-slip rolls [5, 17], $\alpha = 10/13$ for a two-dimensional "monoscale" random flow [8], and various modifications for flows with power-law power spectra [18, 19, 20].

In this paper we revisit the problem of the effective diffusion in laminar Rayleigh-Bénard convection, specifically for hexagonal convection cells with an three-dimensional velocity field [21, 22]. We find that the transport enhancement due to the hexagonal cells is very moderate even at high Péclet numbers, with the scaling function in Eq. (4) being

$$f(P) = \text{const} \ \ln P \ , \quad P \gg 1 \ . \tag{6}$$

The reason for this logarithmic behavior is found in the peculiar geometry of boundary phenomena occuring near the axes and the edges of the hexagons. These peculiarities lead us to introduce the concept of "boundary tubes" reflecting the nature of the diffusion-advection transport in the considered flows. We provide both a scaling (Sec. 2) and numerical (Sec. 3) evidence for the behavior of Eq. (6). In Sec. 4 the regimes of anomalous diffusion in the hexagons where subdiffusion is found for $t < \tau_D$, the diffusion onset time, similar to the subdiffusion found in other flows with constrained streamlines. In Sec. 5 we discuss experimental implications of our results.

2 The logarithmic scaling of effective diffusivity

It is long known [3] that, when the effective diffusivity D^* exists, it expands in a series of even powers of a small Péclet number:

$$D^* = D_0(1 + a_2 P^2 + a_4 P^4 + \ldots) \ , \quad P \ll 1 \ , \tag{7}$$

where $a_2 \geq 0$. On the contrary, in the limit of a large Péclet number, there is no analytic expansion of D^* (although one can devise a continuous fraction instead [23]), because of

the singular nature of *boundary layers* carrying most of the tracer transport. A boundary layer is a region near a separatrix of the velocity field where the two terms in Eq. (2), the advection $\mathbf{v} \cdot \boldsymbol{\nabla} n$ and the molecular diffusion $D_0 \boldsymbol{\nabla}^2 n$, are of the same order.

For example, in free-slip convection rolls with the velocity $\mathbf{v} = \boldsymbol{\nabla}[\psi_0 \sin(\pi x/L) \sin(\pi z/L)] \times \widehat{\mathbf{z}}$ (Fig. 1), the boundary layers are formed near the separatrix $\sin(\pi x/L) \sin(\pi z/L) = 0$. The boundary layer width w is the diffusion distance in the advection turnover time,

$$w = \left(\frac{D_0 L}{v}\right)^{1/2} = L P^{-1/2} , \quad P \gg 1 . \tag{8}$$

Deeper inside the convection roll, the variation of the tracer density n becomes exponentially small, so that the boundary layers are responsible for the effective diffusion. Upon crossing a boundary layer, the particle enters another convection roll thereby completing one step of the random walk between the rolls. Then the effective diffusivity D^* is estimated as the square displacement, L^2, divided by the correlation time, $w^2/D_0 = L/v$, times the fraction $\eta = w/L$ of "active," i.e. residing in the boundary layers, particles. The result is

$$D^* \simeq vw = D_0 P^{1/2} . \tag{9}$$

A more detailed analysis [5, 24, 9] also predicts the numerical factor in (9).

As far as the effective diffusion is concerned, the principal geometrical feature of the convection rolls is that the boundary layers lie near separatrix *surfaces*. Something different occurs in hexagonal Rayleigh-Bénard convection, where the separatrices include (a) the faces between the hexagons, (b) the bissectrices of hexagons' sectors, (c) the edges, and (d) the axes of the hexagons (Fig. 2). In addition to the diffusive ***boundary layers*** formed near *the surfaces* (a) and (b), we expect another kind of boundary phenomenon — *the boundary tubes* — to occur near *the lines* (c) and (d). Specific flow model of the hexagonal convection are presented in Sec. 3 for the purpose of numerical simulation. Here we derive the theoretical scaling law for the effective diffusivity in such a flow.

First we note that, if a tracer particle has crossed a face between two hexagons, it has not yet decorrelated from its Lagrangian history in the sense of completing a step of random walk between the hexagons. Indeed, the topology of the streamlines is such that, upon the advection revolution in the second hexagon, the particle will face the prospect of returning to exactly the same hexagon where its motion started (see Figs. 2 and 3). A complete step of random walk then means entering a third hexagon after multiple sampling of the two neighboring cells. The only way the particle can do so is to diffuse around an edge or an axis of the convection pattern through an angle of order one. Hence the most active particles are those lying in the boundary tubes with the wi . (8) around the edges d the axes, as well as in the volume projected from the bounda.. tubes by the streamlines. Suppose for simplicity that the characteristic scale of the convection cells, L, is the same in both vertical and horizontal directions. If we repeat the previous argument, $D^* \simeq \eta L^2/(w^2/D_0)$, but adjust the fraction of active particles, $\eta \simeq w^2/L^2$, to reflect the tube (versus layer) geometry, a surprising result is inferred: $D^* \simeq D_0$. That is, even for a large Péclet number there is no transport enhancement! Further analysis is required to refine this lowest order conclusion.

In the argument given in the preceding paragraph not all active particles were taken into account. Indeed, because of the incompressible nature of the fluid flow, the streamline projections of the w boundary tubes are much thinner, $w' \simeq w^2/L = L/P$, than the tubes themselves (Fig. 2). This makes the particles penetrate deeper inside the cells by way of diffusing across the streamlines where the layers are thinner (away from the edges and the axes — that is, near the bottom and the surface of the fluid). There, the particles propagate the distance $w \gg w'$ inside the cells during one pass. Then these particles are advected to fill wider boundary tubes with the radius

$$W \simeq (wL)^{1/2} = LP^{-1/4} , \tag{10}$$

near the axes of the hexagons. It is these wider tubes with the radius (10) which contain all

the active particles. It is important that only the vertical component of the small diffusive displacement of a particle near the hexagon bases is significantly amplified by the convection in terms of a much larger radial displacement near the axis; the horizontal component of the displacement near the bases has no effect.

To obtain the refined scaling law for the effective diffusivity, one can pursue the test-particle argument. However, we find it easier to proceed in terms of conductivity, because the problems of conduction and diffusion are mathematically equivalent. We start by noting that the effect of a fast convection is to level out the tracer density along the closed streamlines, so that the two-dimensional diffusion across these lines is only relevant [17, 8]. We wish to represent the transport properties of the array of convection cells as a resistor network with appropriate "diffusive resistances." In Fig. 3 we depict such a network with resistive blobs near the axes of the hexagons connected by good conductors corresponding to the regions where the diffusive resistance is small. Specifically, the horizontal projections of the streamlines are tangential to the faces near the edges of the hexagons. This makes the corresponding boundary tubes easily permeable for the tracer diffusing between the two adjacent sectors of the neighboring cells. We therefore mark the two sectors by a single good conductor (thick segment in Fig. 3). The near-axis boundary tubes, on the contrary, are rotationally invariant. Hence, unlike near the edges, those tubes by no means facilitate the angular diffusion of the tracer and present the principal diffusive resistivity dominating the long-range conduction of the network.

So we calculate the diffusive conductance of of the near-axis boundary tube with the radius W. As the streamlines are almost vertical within the tubes, the cross-streamline diffusion is two-dimensional in the horizontal plane; however, this diffusion is anisotropic. In the azimuthal direction θ (around the axis) the diffusivity is purely molecular, $D_{\theta\theta} = D_0$. In the radial direction the cross-streamline diffusion is much faster, $D_{rr} \simeq W^2/\tau_v = D_0 P^{1/2}$, because a tracer particle is radially displaced through the distance of order W in the

revolution time $\tau_v = L/v$ due to the vertical diffusive deviations from the streamline near the bases of the hexagon. It is emphasized that such a representation of the two-dimensional anisotropic diffusion is valid only for radii $w < r < W$. Now, to formulate the problem in terms of conductivity, we can imagine the good conductors of Fig. 3 to be inserted into the resistive tubes, with the radius W and the azimuthal conductivity D_0, through the radius w. Then the conductance between two adjacent "electrodes" is found from the standard rule of "conductivity times width divided by gap," supplemented by the additivity property for a parallel connection:

$$D_0 \int_w^W \frac{dr}{r} = D_0 \ln W/w \ . \tag{11}$$

The effective conductivity of the network in Fig. 3 is clearly of the same order. So the effective diffusivity of the system of steady Rayleigh-Bénard hexagons scales as

$$D^* \simeq D_0 \ln P \ , \quad P \gg 1 \ . \tag{12}$$

Bearing in mind the extension to anomalous diffusion (Sec. 4), it is instructive to rederive the scaling law (12) using a test-particle argument incorporating the presence of two very different scales, w and W, in the geometry of the boundary tubes. To do so, we subdivide the interval $[w, W]$ into $\log_2(W/w)$ octaves, $[w, 2w]$, $[2w, 4w]$, ..., $[W/2, W]$, and sum the effective diffusivities D_i contrubuted by each octave. The decorrelation time of particles in the ith octave is of order the diffusion time through the radius $r_i = w2^i$: $\tau_i \simeq r_i^2/D_0$. Thus we write

$$D_i \simeq \eta_i L^2/\tau_i \ , \tag{13}$$

where the fraction of volume $\eta_i \simeq r_i^2/L^2$. Then equation (13) evaluates to $D_i \simeq D_0$, and in the sum $D^* = \sum_i D_i$ all terms are of the same order D_0. Thus we recover the logarithmic scaling of the effective diffusivity (12).

The estimate (12) does not require the convection cells to be necessarily hexagonal. The same scaling is valid for any other convection topology, where boundary tubes present the

bottleneck of effective diffusion, such as in square convection cells [25, 26].

3 Numerical results

In this section we report on the numerical investigation of the passive advection-diffusion in hexagonal convection cells. The scaling law (12) of the effective diffusivity is confirmed.

We use the Chandrasekhar [21] representation of the velocity field,

$$v_z(\mathbf{x}) = \frac{u(z)}{3} \sum_{i=1}^{3} \cos(\mathbf{q}_i \cdot \mathbf{x}) \ , \tag{14}$$

$$\mathbf{v}_\perp(\mathbf{x}) = \frac{1}{q^2} \boldsymbol{\nabla}_\perp \frac{\partial v_z}{\partial z} \ , \tag{15}$$

where the vectors $\mathbf{q}_i$ form an equilateral triangle in the (x, y) plane with the side

$$q = \frac{4\pi}{3L} \ , \tag{16}$$

L being the side of the hexagons (Fig. 2). The z-dependence of the velocity field for a free-free boundary condition is given by

$$u(z) = v_0 \sin\left(\frac{\pi z}{h}\right) \ , \tag{17}$$

where h is the depth of the fluid. Other boundary conditions, such as rigid-rigid or rigid-free, lead to modifications in the vertical velocity profile (17) as given in Ref. [21].

The velocity field (14)–(15) can be represented in terms of a vector potential, $\mathbf{v} = \boldsymbol{\nabla} \times \boldsymbol{\psi}$:

$$\boldsymbol{\psi}(\mathbf{x}) = \frac{1}{q^2} \boldsymbol{\nabla} v_z(\mathbf{x}) \times \hat{\mathbf{z}} \ . \tag{18}$$

Then the Péclet number can be introduced in the standard way as

$$P \equiv \frac{\left\langle \boldsymbol{\psi}^2(\mathbf{x}) \right\rangle^{1/2}}{D_0} = \frac{\sqrt{3}}{8\pi} \frac{L v_0}{D_0} \ . \tag{19}$$

We computed $N = 1000$ particle orbits in the flow (14)–(15) with $v_0 = L = h = 1$ using the standard Runge-Kutta fourth-order integrator with the fixed time step $\Delta t = 0.1$.

Initially, the particles were distributed on a circle with the radius 0.01 encompassing the middle of the axis of one of the hexagons. After each step of the integration the particles were randomly displaced at the distance of $\pm(2D_0\Delta t)^{1/2}$ in each Cartesian direction, which models the molecular diffusion D_0. When a particle reached the bottom $z = 0$ or the surface $z = h$ of the fluid, it was reflected from the boundary by reversing the sign of the diffusive displacement. Figure 4 presents the distribution of particles at a time when the effective diffusion has set in.

The effective diffusion in the (x, y) plane is measured by the usual expression

$$D^*(t) = \frac{1}{4t} \sum_{i=1}^{N} \left([x_i(t) - x_i(0)]^2 + [y_i(t) - y_i(0)]^2 \right) . \tag{20}$$

as it saturates with time (also shown in Fig. 4). The dependence of the diffusivity enhancement $D^*(\infty)/D_0$ on the Péclet number (19) is shown in Fig. 5 in semi-logarithmic axes. The approximately linear dependence of D^*/D_0 on $\ln P$, as well as the very modest diffusion enhancement even for $P = 10^3$ and more, support the logarithmic scaling (12). In the notation of Eq. (19) for free-free hexagonal convection we numerically infer

$$D^* = D_0(0.58 \ln P + 0.85) , \quad 30 < P < 1000 , \tag{21}$$

with an approximately 3% error margin.

4 Anomalous diffusion

The effective diffusion regime sets in only after a certain mixing time τ_D, corresponding to the tracer particles diffusively sampling all of a convection cell:

$$\tau_D = \frac{L^2}{D_0} = \tau_v P , \tag{22}$$

where $\tau_v = L/v$ is the characteristic convection time. For this reason the computation of the effective diffusion gets progressively expensive for higher Péclet numbers. On the

intermediate time scales, $\tau_v \ll t \ll \tau_D$, the tracer transport can be anomalous, i.e. sub- or superdiffusive [17, 19]. In the case of a "monoscale" flow with a bounded vector potential, only subdiffusion is possible [20]. In this section we derive the subdiffusive scaling law for convection cells with boundary tubes.

A well-distinguished subdiffusion takes place only for a special initial condition, namely when the tracer is initially at or near the separatrices. In the case of thermal convection this condition is easily satisfied by placing the tracer at the bottom or the surface of the fluid. The origin of the anomalous diffusion comes from the change with time of the fraction of "active" particles $\eta(t)$.

The test-particle argument of Sec. 2 can be adjusted to allow for the transient effect of filling up the interiors of the convection cells. The octave of radii $[w_i, 2w_i]$ (where $w_i = w2^i$) within a boundary tube corresponds to the volume $V_i \simeq w_i^2 L$. The total volume invaded by the tracer particles by the time t is $V(t) \simeq L^2(D_0 t)^{1/2}$, $\tau_v < t < \tau_D$, because the invasion primarily occurs near the bottom and the surface where the width of a flow flux tube is narrower. Hence we have the fraction of particles residing in the ith partition of the boundary tube:

$$\eta_i(t) = \frac{V_i}{V(t)} = \frac{w_i^2}{L(D_0 t)^{1/2}} , \quad \tau_v < t < \tau_D . \tag{23}$$

As time exceeds the mixing time τ_D, $\eta_i(t)$ saturates at approximately $\eta_i(\tau_D)$; however, on the intermediate time scales $\eta_i(t)$ behaves algebraicaly and leads to the anomalous diffusion.

Now we write an estimate for the moments of the tracer distribution using a straightforward generalization of Eq. (13):

$$\left\langle [\mathbf{x}(t) - \mathbf{x}(0)]^{2m} \right\rangle \simeq \sum_{i=1}^{\log_2(W/w)} \eta_i(t) \left(\frac{L^2}{w_i^2/D_0} t \right)^m . \tag{24}$$

Upon substituting Eq. (23) we finally infer

$$\left\langle [\mathbf{x}(t) - \mathbf{x}(0)]^{2m} \right\rangle^{1/m} \simeq \begin{cases} L^2 \ln P (D_0 t)^{1/2} , & m = 1 , \\ L^2 P^{1-1/m} (D_0 t / L^2)^{1-1/(2m)} , & m > 1 , \end{cases} \tag{25}$$

a subdiffusive scaling law. The $m = 1$ scaling $\langle x^2 \rangle \propto t^{1/2}$ corresponds to the usual "double diffusion" encountered in covection rolls with free-slip boundary conditions [27].

We did not attempt to study this transient transport regime numerically, because it would require a very small time step Δt in order to resolve the diffusive invasion of the tracer near the hexagon bases. There, the streamline projection of the w boundary tube is only $w' = w^2/L = L/P$ thick. The resolution requirement $\delta = (D_0 \Delta t)^{1/2} \ll w'$ would then result in $\Delta t \ll \tau_v/P$, which is unrealistic for a particle-method computation of the advection-diffusion transport. There appear to be, though, no principal difficulties of studying the anomalous diffusion experimentally [6, 7].

5 Conclusion

We generalize the concept of an advection-diffusion boundary layer to three-dimensional geometries, where the separatrices can be both surfaces and lines. In the second case, relevant for hexagonal or square thermal convection, the boundary tubes occurring near the axes of the cells, due to the three-dimensional accumulation of incompressible streamlines, act as the bottleneck for passive transport. This leads to a new logarithmic scaling (12) for the effective diffusivity, showing an anomalously weak transport enhancement in comparison with what is found in convection rolls and other geometries.

The anomalously weak transport enhancement may present a new interesting experimental opportunity. The logarithmic diffusivity scaling (12) relies on (a) the presense of boundary tubes and (b) closed streamlines. Any small perturbation to this flow, such as oscillations of the convection pattern or the appearance of a "swirl," whereby the streamlines wind around flux surfaces and the particles are *advected* round the cells' axes [26], can drastically enhance the effective diffusivity and lead to a scaling similar to Eq. (9), with an extra factor involving the intensity of the swirl. These measurable/visualizable effects can be used to study the fine internal structure of convection patterns and transitions between

the patterns.

Acknowledgments

We would like to acknowledge stimulating discussions with H. L. Swinney, M. Schatz, and A. A. Chernikov. This work was supported by the U.S. Department of Energy under Contract No. DE-FG05-80ET53088.

References

[1] G. I. Taylor. Diffusion by continuous movements. *Proc. Lond. Math. Soc. Ser. 2*, 20:196, 1921.

[2] L. F. Richardson. Atmospheric diffusion shown on a distance-neighbor graph. *Proc. R. Soc. London Ser. A*, 110:709, 1926.

[3] Ya. B. Zeldovich. Limiting laws for free upwelling convective flows. *Dokl. Akad. Nauk SSSR*, 7:1466, 1937. In Russian.

[4] G. I. Taylor. Dispersion of soluble matter in solvent flowing slowly through a tube. *Proc. R. Soc. London Ser. A*, 219:186, 1953.

[5] M. N. Rosenbluth, H. L. Berk, I. Doxas, and W. Horton. Effective diffusion in laminar convective flows. *Phys. Fluids*, 30:2636, 1987.

[6] T. H. Solomon and J. P. Gollub. Passive transport in steady Rayleigh-Bénard convection. *Phys. Fluids*, 31:1372, 1988.

[7] O. Cardoso and P. Tabeling. Anomalous diffusion in a linear array of vortices. *Europhys. Lett.*, 7:225, 1988.

[8] M. B. Isichenko, J. Kalda, E. B. Tatarinova, O. V. Telkovskaya, and V. V. Yankov. Diffusion in a medium with vortex flow. *Zh. Eksp. Teor. Fiz.*, 96:913, 1989. [English transl. Sov. Phys. JETP **69**, 517 (1989)].

[9] M. V. Osipenko, O. P. Pogutse, and N. V. Chudin. Plasma diffusion in an array of vortices. *Fiz. Plazmy*, 13:953, 1987. [English transl. Sov. J. Plasma Phys. **13**, 550 (1987)].

[10] K. V. Chukbar and V. V. Yankov. Evolution of the magnetic field in plasma opening switches. *Zh. Tekhn. Fiz.*, 58:2130, 1988. [English transl. Sov. Tech. Phys. **33**, 1293 (1988)].

[11] H. K. Moffatt. Transport effects associated with turbulence with particular attention to the influence of helicity. *Rep. Prog. Phys.*, 46:621, 1983.

[12] A. M. Soward. Fast dynamo action in a steady flow. *J. Fluid Mech.*, 180:267, 1987.

[13] Yu. A. Dreizin and A. M. Dykhne. Anomalous conductivity of inhomogeneous media in a strong magnetic field. *Zh. Eksp. Teor. Fiz.*, 63:242, 1972. [English transl. Sov. Phys. JETP **36**, 127 (1973)].

[14] M. B. Isichenko and J. Kalda. Anomalous resistance of randomly inhomogeneous Hall media. *Zh. Eksp. Teor. Fiz.*, 91:224, 1991. [English transl. Sov. Phys. JETP **72**, 126 (1991)].

[15] M. Avellaneda and A. J. Majda. Stieltjes integral representation and effective diffusivity bounds for turbulent transport. *Phys. Rev. Lett.*, 62:753, 1989.

[16] E. B. Tatarinova, P. A. Kalugin, and A. V. Sokol. What is the propagation rate of the passive component in turbulent flows limited by? *Europhys. Lett.*, 14:773, 1991.

[17] W. R. Young, A. Pumir, and Y. Pomeau. Anomalous diffusion of tracer in convection rolls. *Phys. Fluids A*, 1:462, 1989.

[18] D. L. Koch and J. F. Brady. Anomalous diffusion due to long-range velocity fluctuations in the absence of a mean flow. *Phys. Fluids A*, 1:47, 1989.

[19] M. B. Isichenko and J. Kalda. Statistical topography. II. 2D transport of a passive scalar. *J. Nonlinear Science*, 1:375, 1991.

[20] M. B. Isichenko. Percolation, statistical topography, and transport in random media. *Rev. Mod. Phys.*, 64(4):961–1043, 1992.

[21] S. Chandrasekhar. *Hydrodynamic and hydromagnetic stability.* Dover, New York, 1961.

[22] F. H. Busse. Nonlinear properties of thermal convection. *Rep. Prog. Phys.*, 41:1929, 1978.

[23] P. A. Kalugin, A. V. Sokol, and E. B. Tatarinova. Analytical properties of the effective-diffusion coefficient in periodic flows. *Europhys. Lett.*, 13:417, 1990.

[24] B. Shraiman. Diffusive transport in Rayleigh-Bénard convection cell. *Phys. Rev. A*, 36:261, 1987.

[25] W. V. R. Malkus and G. Veronis. *J. Fluid Mech.*, 4:225, 1957.

[26] A. A. Chernikov and G. Schmidt. Chaotic streamlines in convective cells. *Phys. Lett. A*, 169:51–56, 1992.

[27] Y. Pomeau, A. Pumir, and W. R. Young. Transitoires dans l'advection-diffusion d'impuretés. *C. R. Acad. Sci. (Paris)*, 306 II:741, 1988.

Figure Captions

1. Schematic of convection rolls. The boundary layers (shown hatched) have approximately the same width w away from the stagnation points.

2. Schematic of hexagonal convection. Two neighboring hexagons are shown. The topology of the flow is such that there are two types of boundary layers [(a) and (b)] and two types of boundary tubes [(c) and (d)]. The projections of the boundary tubes (width W) along the streamlines are much narrower ($w \simeq W^2/L$) near the bottom and the surface of the fluid, where the molecular diffusion has the most significant effect.

3. Schematic of advection-diffusion transport in hexagonal convection. The shaded curves show the horizontal projections of the streamlines specified by Eqs. (14) and (15). Due to the tangential behavior of the streamlines at the faces of the hexagons, the "diffusive resistance" between the two adjacent sectors is small, compared to D_0^{-1}, as a power of the Péclet number, and is represented by a good conductor (shown in bold segments). The principal diffusive resistance is concentrated in the boundary tubes (shown by circles with the radii w and W) near the axes of the hexagons.

4. The distribution of particles seen from different prospectives (a)–(c) and the time behavior of the effective diffusivity (20) (d): shows that $D^*(t)$ saturates to a constant in about the mixing time (22).

5. The diffusion enhancement D^*/D_0, due to the steady hexagonal convection, plotted against the Péclet number P.

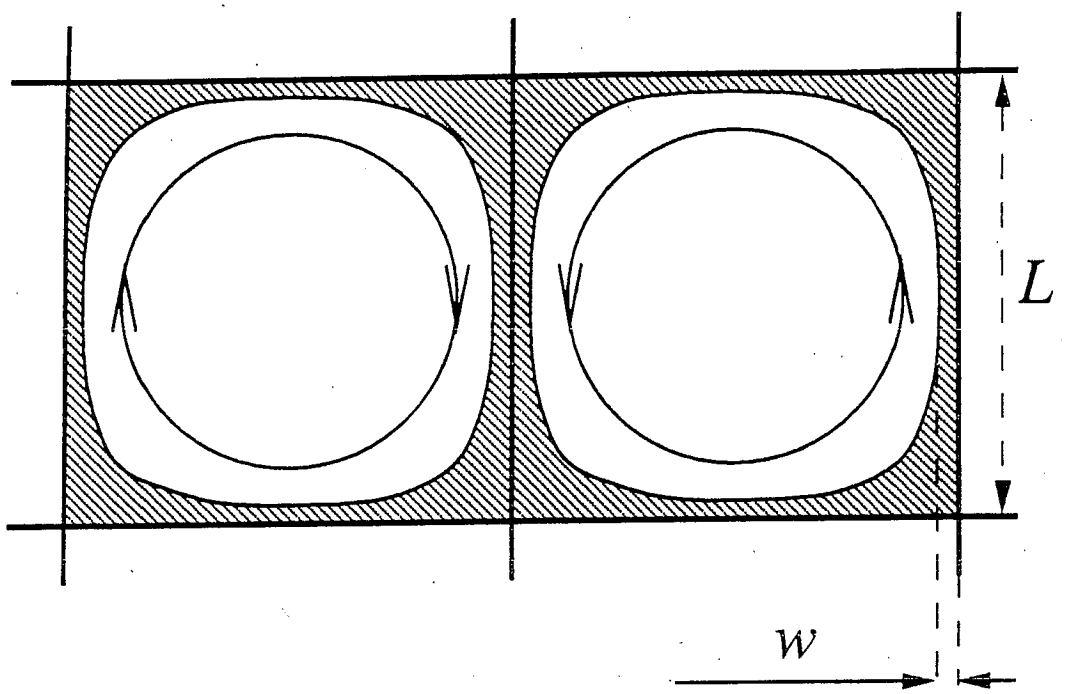

Figure 1.

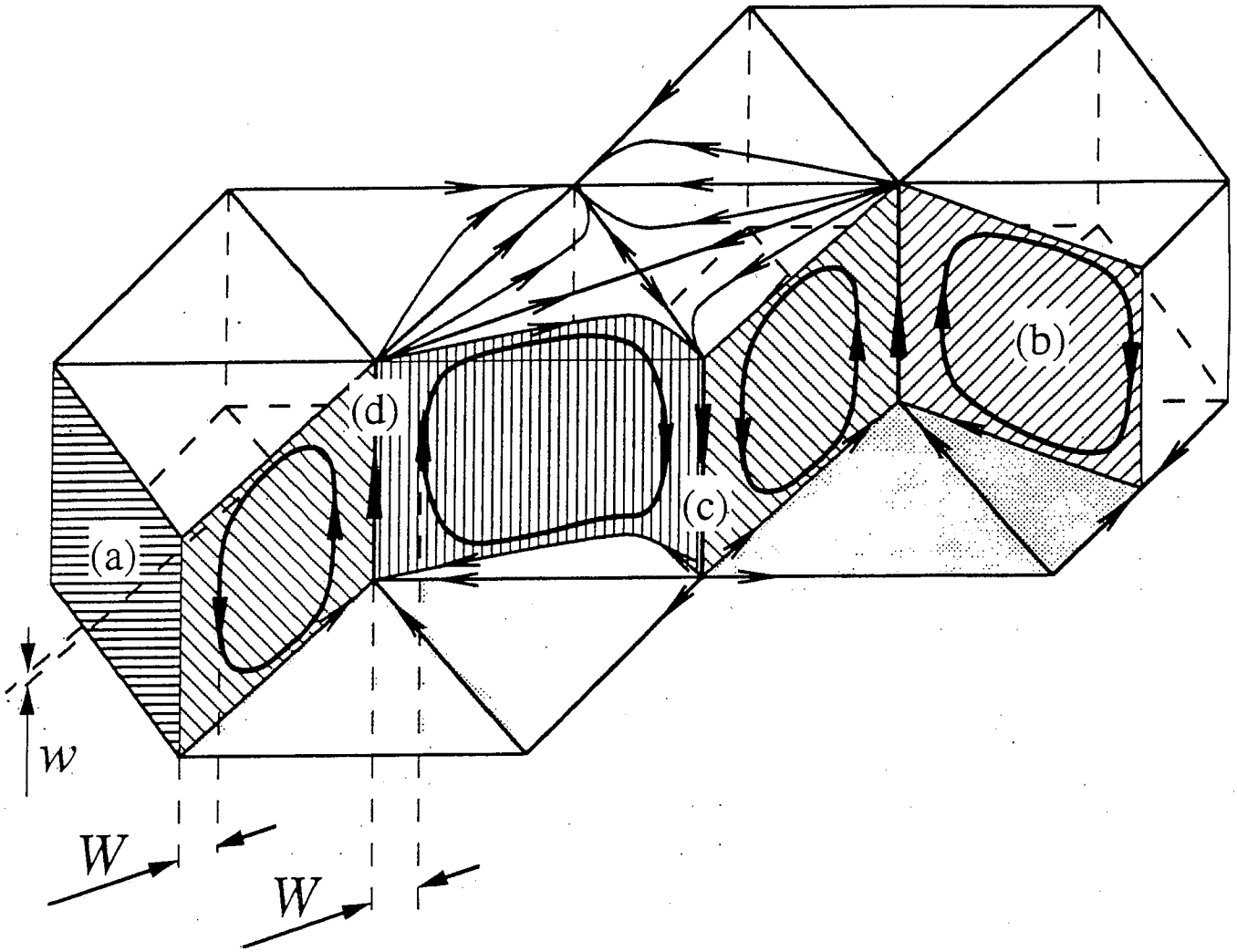

Figure 2.

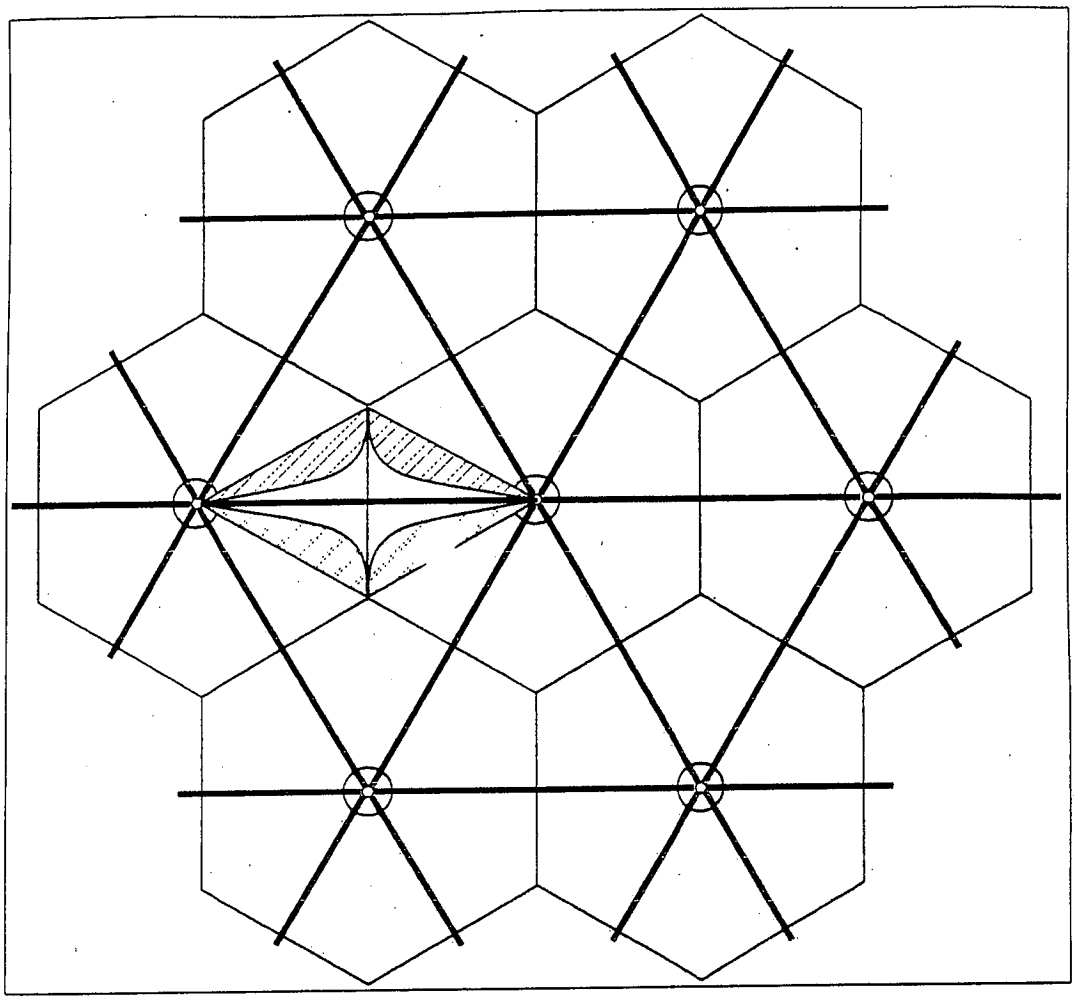

Fig. 3

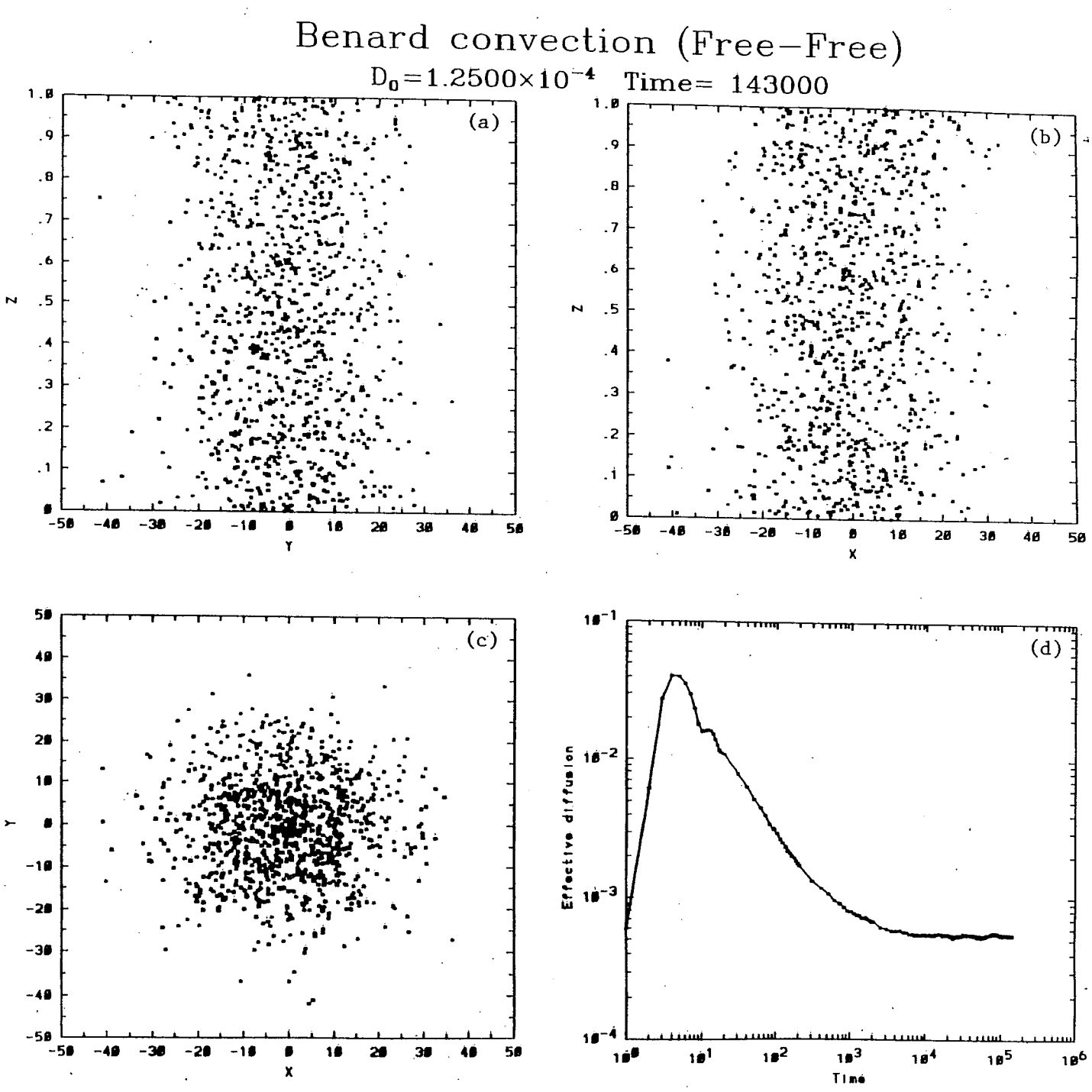
Benard convection (Free-Free)
D_0=1.2500×10^{-4} Time= 143000
(a)
(b)
(c)
(d)
Z
Y
X
Effective diffusion
Time

Fig. 4

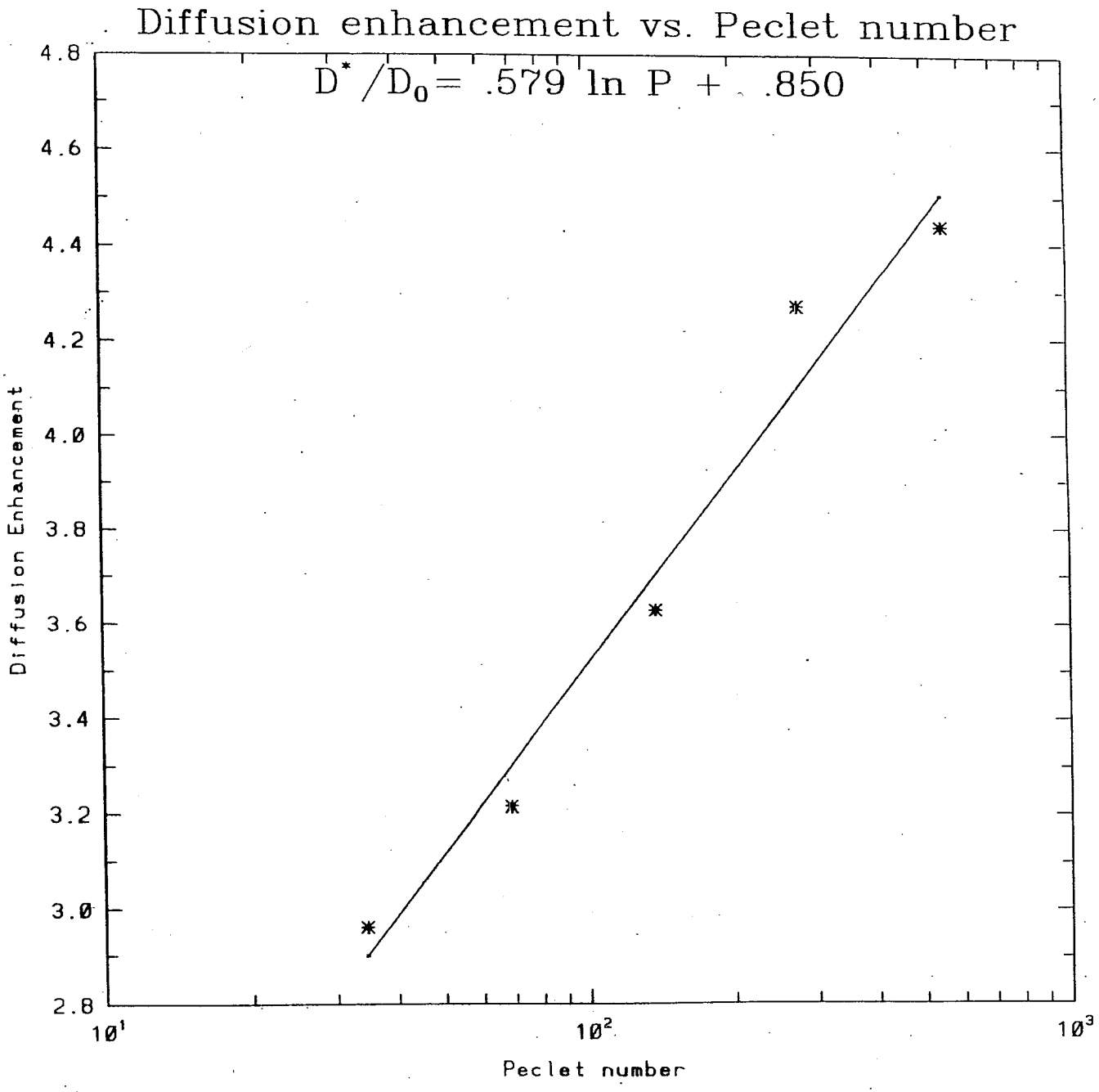
Diffusion enhancement vs. Peclet number
$D^*/D_0 = .579 \ln P + .850$
Diffusion Enhancement
4.8
4.6
4.4
4.2
4.0
3.8
3.6
3.4
3.2
3.0
2.8
10^1
10^2
10^3
Peclet number

Fig. 5